

Constraints on Ξ^- nuclear interactions from capture events in emulsion

E. Friedman, A. Gal*

Racah Institute of Physics, The Hebrew University, Jerusalem 91904, Israel

Abstract

Five $\Xi^-p \rightarrow \Lambda\Lambda$ two-body capture events in ^{12}C and ^{14}N emulsion nuclei, in which a pair of single- Λ hypernuclei is formed and identified by their weak decay, have been observed in (K^-, K^+) emulsion exposures at KEK and J-PARC. Applying a Ξ^- -nucleus optical potential methodology to study atomic and nuclear transitions, we confirm that these capture events occur from Coulomb assisted $1p_{\Xi^-}$ nuclear states. Long-range ΞN shell-model correlations are found essential to achieve consistency between the ^{12}C and ^{14}N events. The resulting Ξ -nuclear interaction is strongly attractive, with Ξ potential depth in nuclear matter $V_{\Xi} \gtrsim 20$ MeV. Implications to multi-strangeness features of dense matter are outlined.

Keywords: hyperon strong interactions; Ξ^- atoms and hypernuclei.

1. Introduction and background

Recent two-particle correlation studies of $p\Lambda$, $\Lambda\Lambda$ and Ξ^-p pairs measured by ALICE [1, 2, 3, 4] in pp and p -Pb ultra-relativistic collisions at TeV energies have triggered renewed interest in Strangeness $\mathcal{S} \neq 0$ baryon-baryon interactions and consequences thereof to strange hadronic matter. In particular, the Ξ^-p interaction was shown to be attractive [3], in good agreement with the recent HAL-QCD lattice calculations reaching $m_{\pi} = 146$ MeV [5]. Understanding the strength of the $\mathcal{S} = -2$ ΞN interaction, particularly when embedded in nuclear media, is vital for resolving the Hyperon Puzzle which addresses the fate of hyperons in dense neutron-star matter [6].

*corresponding author: Avraham Gal, avragal@savion.huji.ac.il

Little is known from experiment on the nuclear interaction of Ξ hyperons [7, 8]. A standard reaction production is the nuclear (K^-, K^+) reaction, driven by $K^-p \rightarrow K^+\Xi^-$ strangeness exchange on protons. Owing to its large momentum transfer, the produced Ξ^- hyperons populate dominantly the quasi-free continuum region, with less than 1% expected to populate Ξ^- -nuclear bound states that decay subsequently by the $\Xi^-p \rightarrow \Lambda\Lambda$ strong-interaction capture reaction. Analysis of old emulsion events attributed to the formation of Ξ hypernuclei suggested attractive Woods-Saxon Ξ nuclear potential depth $V_{\Xi}=21\text{-}24$ MeV [9]. While this range of values is considered sufficient for Ξ hyperons to play an active role in strange hadronic matter [10] and in neutron stars [11], somewhat smaller values follow from studies of dedicated (K^-, K^+) counter experiments: $V_{\Xi} \lesssim 20$ MeV in KEK PS-E224 [12], $V_{\Xi} \sim 14$ MeV in BNL AGS-E885 [13], both on ^{12}C , and $V_{\Xi} = 17 \pm 6$ MeV on ^9Be [14] from BNL AGS-E906 [15]. New results from the J-PARC E05 and E70 (K^-, K^+) experiments on ^{12}C are forthcoming [16]. However, no Ξ^- or $\Lambda\Lambda$ hypernuclear bound states have ever been observed unambiguously in these experiments. Powerful future experiments by the PANDA Collaboration at FAIR [17], using $\bar{p}p \rightarrow \Xi^-\bar{\Xi}^+$ or $\bar{p}n \rightarrow \Xi^-\bar{\Xi}^0$ production modes, and also at BESIII [18] focusing on the $J/\psi \rightarrow \Xi^-\bar{\Xi}^+$ $O(10^{-3})$ decay branch, are likely to change this state of the art.

The situation is different in exposures of light-emulsion CNO nuclei to the (K^-, K^+) reaction, in which a tiny fraction of the produced high-energy Ξ^- hyperons slow down in the emulsion, undergoing an Auger process to form high- n atomic levels, and cascade down radiatively. Cascade essentially terminates, when strong-interaction capture takes over, in a 3D atomic state bound by 126, 175, 231 keV in C, N, O, respectively. The 3D strong-interaction shift is less than 1 keV [19]. Capture events are recorded by observing Λ hyperon or hypernuclear decay products. Interestingly, whereas the few observed double- Λ hypernucleus production events are consistent with Ξ^- capture from atomic 3D states [8], formation of pairs of single- Λ hypernuclei requires capture from a lower Ξ^- orbit. Expecting the final two Λ hyperons in $\Xi^-p \rightarrow \Lambda\Lambda$ capture to be formed in a $S = 0, 1s_{\Lambda}^2$ configuration, the initial Ξ^- hyperon and the proton on which it is captured must satisfy $l_{\Xi^-} = l_p$ [20] which for p -shell nuclear targets favors the choice $l_{\Xi^-} = 1$. Indeed, all two-body Ξ^- capture events, $\Xi^- + {}^AZ \rightarrow {}^{A'}_{\Lambda}Z' + {}^{A''}_{\Lambda}Z''$, to twin single- Λ hypernuclei reported from KEK and J-PARC light-emulsion K^- exposures [21, 22, 23], as listed here in Table 1, are consistent with Ξ^- capture from Coulomb-assisted $1p_{\Xi^-}$ nuclear states bound by ~ 1 MeV.

Table 1: Reported two-body Ξ^- capture events $\Xi^- + {}^A Z \rightarrow {}^{A'}_{\Lambda} Z' + {}^{A''}_{\Lambda} Z''$ in light-emulsion nuclei to a pair of single- Λ hypernuclei, some in ground states, some in specific excited states marked by asterisk. Only the first and last events are uniquely assigned. Fitted Ξ^- binding energies B_{Ξ^-} are listed.

Experiment	Event	${}^A Z$	${}^{A'}_{\Lambda} Z' + {}^{A''}_{\Lambda} Z''$	B_{Ξ^-} (MeV)
KEK E176 [21]	10-09-06	${}^{12}\text{C}$	${}^4_{\Lambda}\text{H} + {}^9_{\Lambda}\text{Be}$	0.82 ± 0.17
KEK E176 [21]	13-11-14	${}^{12}\text{C}$	${}^4_{\Lambda}\text{H} + {}^9_{\Lambda}\text{Be}^*$	0.82 ± 0.14
KEK E176 [21]	14-03-35	${}^{14}\text{N}$	${}^3_{\Lambda}\text{H} + {}^{12}_{\Lambda}\text{B}$	1.18 ± 0.22
KEK E373 [22]	KISO	${}^{14}\text{N}$	${}^5_{\Lambda}\text{He} + {}^{10}_{\Lambda}\text{Be}^*$	1.03 ± 0.18
J-PARC E07 [23]	IBUKI	${}^{14}\text{N}$	${}^5_{\Lambda}\text{He} + {}^{10}_{\Lambda}\text{Be}$	1.27 ± 0.21

In Table 1 only the first and last listed events are uniquely assigned in terms of initial emulsion nucleus ${}^A Z$ and final single- Λ hypernuclei ${}^{A'}_{\Lambda} Z' + {}^{A''}_{\Lambda} Z''$ ground states, providing thereby a unique value of B_{Ξ^-} per each event. The events fitted by assuming specific excited states ${}^{A''}_{\Lambda} Z''^*$ are equally well fitted each by g.s. assignments ${}^{A''}_{\Lambda} Z''$, with values of B_{Ξ^-} as high as ~ 4 MeV, and the middle event is equally well fitted as a capture event in ${}^{16}\text{O}$, to ${}^3_{\Lambda}\text{H} + {}^{14}_{\Lambda}\text{C}$ with $B_{\Xi^-} = 0.46 \pm 0.39$ MeV or to ${}^4_{\Lambda}\text{H} + {}^{13}_{\Lambda}\text{C}$ with $B_{\Xi^-} = 0.40 \pm 0.27$ MeV, both consistent with Ξ^- capture from an atomic 3D state. We note that the listed Ξ^- binding energy B_{Ξ^-} values are all around 1 MeV, significantly higher than the purely-Coulomb atomic 2P binding energy values which are approximately 0.3, 0.4, 0.5 MeV in C,N,O atoms, respectively. These ~ 1 MeV B_{Ξ^-} values correspond to $1p_{\Xi^-}$ nuclear states that evolve from 2P atomic states upon adding a strong-interaction Ξ nuclear potential.¹ This interpretation is the only one common to *all* five events.

Not listed in the table are multi-body capture events that require for their interpretation undetected capture products, usually neutrons, on top of a pair of single- Λ hypernuclei. Most of these new J-PARC E07 events [24] imply Ξ^- capture from $1s_{\Xi^-}$ nuclear states, with capture rates $\mathcal{O}(10^{-2})$ of capture rates from the $1p_{\Xi^-}$ nuclear states considered here [20, 25].

In the present work we consider Ξ^- atomic and nuclear transitions in light emulsion atoms, first with a $t\rho$ optical potential, to substantiate that

¹Nuclear single-particle (s.p.) states are denoted by lower-case letters: $1s, 1p, 1d, \dots$ for the lowest l values, in distinction from atomic s.p. states denoted by capitals: $1S, 2P, 3D, \dots$ for the lowest L values.

$\Xi^- p \rightarrow \Lambda\Lambda$ capture indeed occurs from a Coulomb-assisted nuclear $1p_{\Xi^-}$ state in light emulsion nuclei. The strength of this Ξ -nuclear potential is determined by requiring that it reproduces a $1p_{\Xi^-}$ state in $^{12}\text{C}(0_{\text{g.s.}}^+)$ bound by 0.82 ± 0.15 MeV from Table 1. Disregarding temporarily the $s_{\Xi^-} = \frac{1}{2}$ Pauli-spin degree of freedom, we proceed to discuss the implications of identifying the value $B_{\Xi^-} \approx 1.15 \pm 0.20$ MeV for ^{14}N from Table 1 with the binding energy of $\mathcal{L}^\pi = (0^-, 1^-, 2^-)$ triplet of $1p_{\Xi^-}$ nuclear states built on $J^\pi(^{14}\text{N}_{\text{g.s.}}) = 1^+$, thereby linking the capture process to properties of the Ξ -nucleus residual interaction. This provides the only self consistent deduction of the Ξ -nuclear interaction strength from analysis of the five Ξ^- capture events in light nuclear emulsion, fitted to two-body formation of specific Λ hypernuclei, as listed in Table 1. The resulting $t\rho$ Ξ potential depth at nuclear-matter density $\rho_0 = 0.17 \text{ fm}^{-3}$ is $V_{\Xi} \approx 24$ MeV. We then improve upon the $t\rho$ leading term of the optical potential by introducing the next, Pauli correlation term in the optical potential density expansion [26]. This leads to $\approx 10\%$ reduction of V_{Ξ} , down to $V_{\Xi} \approx 22$ MeV, keeping it within the optical potential approach well above 20 MeV. Our results suggest that $1s_{\Xi^-}$ nuclear bound states exist all the way down to ^4He , with potentially far-reaching implications for the role of Ξ hyperons in multi-strange dense matter.

A value $V_{\Xi} \gtrsim 20$ MeV implies a substantially stronger in-medium ΞN attraction than reported by some recent model evaluations (HAL-QCD [27], EFT@NLO [28, 29], RMF [30]) all of which satisfy $V_{\Xi} \lesssim 10$ MeV. A notable exception is provided by versions ESC16*(A,B) of the latest Nijmegen extended-soft-core ΞN interaction model [31], in which values of V_{Ξ} higher than 20 MeV are derived. However, these large values are reduced substantially by ΞNN three-body contributions within the same ESC16* model.

2. Methodology

The starting point in optical-potential analyses of hadronic atoms [32] is the in-medium hadron self-energy $\Pi(E, \vec{p}, \rho)$ that enters the in-medium hadron (here Ξ hyperon) dispersion relation

$$E^2 - \vec{p}^2 - m_{\Xi}^2 - \Pi(E, \vec{p}, \rho) = 0, \quad (1)$$

where \vec{p} and E are the Ξ momentum and energy, respectively, in nuclear matter of density ρ . The resulting Ξ -nuclear optical potential V_{opt} , defined by $\Pi(E, \vec{p}, \rho) = 2EV_{\text{opt}}$, enters the near-threshold Ξ^- wave equation

$$[\nabla^2 - 2\mu(B + V_{\text{opt}} + V_c) + (V_c + B)^2] \psi = 0, \quad (2)$$

where $\hbar = c = 1$. Here μ is the Ξ^- -nucleus reduced mass, B is the complex binding energy, V_c is the finite-size Coulomb potential of the Ξ^- hyperon with the nucleus, including vacuum-polarization terms, all added according to the minimal substitution principle $E \rightarrow E - V_c$. Strong-interaction optical-potential V_{opt} terms other than $2\mu V_{\text{opt}}$ are negligible and omitted here. The use of a Klein-Gordon wave equation (2) for the Ξ^- fermion rather than Dirac equation provides an excellent approximation when $Z\alpha \ll 1$ and fine-structure effects are averaged on, as for the X-ray transitions considered here. Ξ^- nuclear spin-orbit effects are briefly mentioned below.

For V_{opt} in Eq. (2) we first use a standard $t\rho$ form [32]

$$V_{\text{opt}}(r) = -\frac{2\pi}{\mu} \left(1 + \frac{A-1}{A} \frac{\mu}{m_N}\right) [b_0\rho(r) + b_1\rho_{\text{exc}}(r)], \quad (3)$$

where the complex strength parameters b_0 and b_1 are effective, generally density dependent ΞN isoscalar and isovector c.m. scattering amplitudes respectively. The density $\rho = \rho_n + \rho_p$ is a nuclear density distribution normalized to the number of nucleons A and $\rho_{\text{exc}} = \rho_n - \rho_p$ is a neutron-excess density with $\rho_n = (N/Z)\rho_p$, implying that $\rho_{\text{exc}} = 0$ for the $N = Z$ emulsion nuclei ^{12}C and ^{14}N analyzed in the next section. Here we used mostly nuclear density distributions of harmonic-oscillator (HO) type [33] where the r.m.s. radius of ρ_p was set equal to that of the known nuclear charge density [34]. Folding reasonably chosen ΞN interaction ranges other than corresponding to the proton charge radius, or using Modified Harmonic Oscillator (MHO) densities, or replacing HO densities by realistic three-parameter Fermi (3pF) density distributions [35, 36] made little difference: all the calculated binding energies changed by a small fraction, about 0.03 MeV of the uncertainty imposed by the ± 0.15 MeV experimental uncertainty of the 0.82 MeV $1p_{\Xi}$ binding energy in ^{12}C listed in Table 1. We note that the central density $\rho(0)$ in all density versions used here is within acceptable values for nuclear matter, i.e., between roughly 0.15 and 0.20 fm^{-3} .

The form of V_{opt} given by Eq. (3) corresponds to a central-field approximation of the Ξ -nuclear interaction. Spin and isospin degrees of freedom induced by the most general two-body s -wave ΞN interaction $V_{\Xi N}$,

$$V_{\Xi N} = V_0 + V_\sigma \sigma_{\Xi} \cdot \sigma_N + V_\tau \tau_{\Xi} \cdot \tau_N + V_{\sigma\tau} \sigma_{\Xi} \cdot \sigma_N \tau_{\Xi} \cdot \tau_N \quad (4)$$

with V s functions of $r_{\Xi N}$, are suppressed in this approach. Choosing $^{12}\text{C}_{\text{g.s.}}$ with isospin $I = 0$ and spin-parity $J^\pi = 0^+$ for a nuclear medium offers

the advantage that only V_0 is operative in leading order since the nuclear expectation value of each of the other three terms in Eq. (4) vanishes. But for $^{14}\text{N}_{\text{g.s.}}$, with $I(J^\pi)=0(1^+)$, V_σ is operative as well, adding unavoidable model dependence of order $\mathcal{O}(1/A)$ to Ξ^- -nuclear potential depth values derived from capture events assigned to this emulsion nucleus. For this reason we start the present analysis with the two Ξ^- - ^{12}C emulsion events of Table 1.

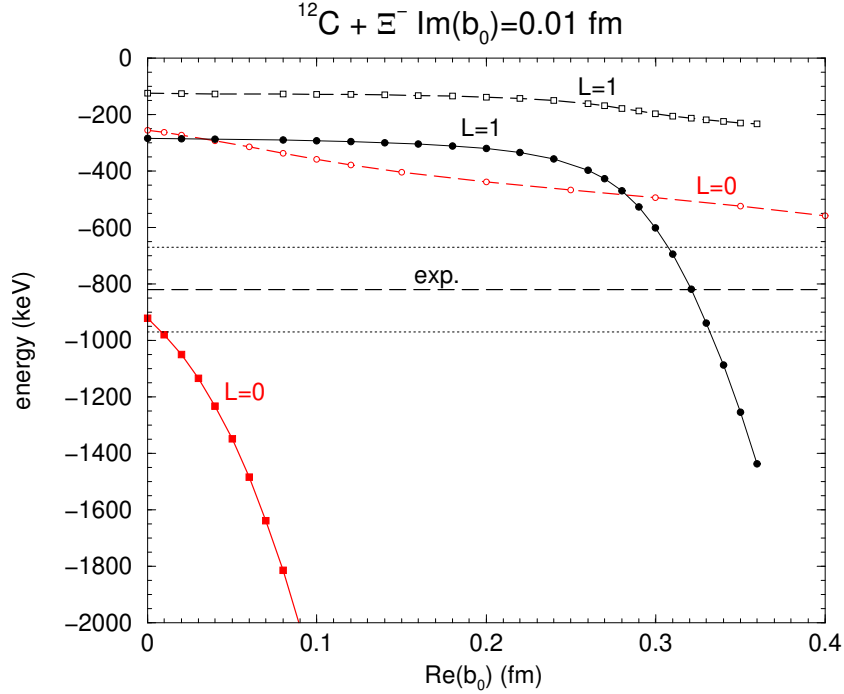


Figure 1: Energy levels (in keV) of the lowest Ξ^- atomic states for $L=0$ (1S,2S) and $L=1$ (2P,3P) in ^{12}C as a function of the strength parameter $\text{Re } b_0$ (in fm) of the Ξ^- optical potential (3). Spin-orbit splittings of $L=1$ states are suppressed in this figure. The dashed and dotted horizontal lines mark the value $B_{\Xi^-} = 0.82 \pm 0.15 \text{ MeV}$ from Table 1.

3. Ξ^- capture in ^{12}C

Figure 1 shows a portion of the combined atomic plus nuclear spectrum of Ξ^- in ^{12}C , $B_{\Xi^-} \leq 2 \text{ MeV}$, as a function of $\text{Re } b_0$, Eq. (3), for a fixed $\text{Im } b_0 = 0.01 \text{ fm}$ corresponding to a nuclear-matter Ξ^- capture width $\Gamma_{\Xi^-} \approx 1.5 \text{ MeV}$, compatible with the HAL-QCD weak $\Xi^- p \rightarrow \Lambda\Lambda$ transition

potential [5]. Plotted are the energies of the two lowest states of each orbital angular momentum $l_{\Xi^-} = 0, 1$, starting at $\text{Re } b_0=0$ with almost purely atomic states 1S,2P,2S,3P from bottom up. Of these states the 1S state with Bohr radius about 3.8 fm is indistinguishable from a nuclear 1s state, and indeed it dives down in energy as soon as $\text{Re } b_0$ is made nonzero. It takes considerable strength, $\text{Re } b_0 \gtrsim 0.25$ fm, before the next atomic state, 2P with Bohr radius about 15 fm, overlaps appreciably with the $^{12}\text{C}_{\text{g.s.}}$ nuclear core, diving down in energy to become a nuclear $1p_{\Xi^-}$ state. The higher two states that start as atomic 2S,3P remain largely atomic as $\text{Re } b_0$ is varied in Fig. 1. Their slowly decreasing energies indicate a rearrangement of the atomic spectrum [37]: $2\text{S} \rightarrow 1\text{S}$ and $3\text{P} \rightarrow 2\text{P}$. Judging by the marked band of values $B_{\Xi^-} = 0.82 \pm 0.15$ MeV for the two KEK E176 events listed in Table 1, the figure suggests that they are compatible with a $1p_{\Xi^-}$ nuclear state corresponding to a Ξ^- -nuclear potential strength of $\text{Re } b_0 = 0.32 \pm 0.01$ fm. The sensitivity to variations of $\text{Im } b_0$ is minimal: choosing $\text{Im } b_0 = 0.04$ fm [19] instead of 0.01 fm increases $\text{Re } b_0$ by 0.01 fm to 0.33 ± 0.01 fm.

Radiative rates for E1 transitions from the Ξ^- atomic 3D state to the Ξ^- atomic 3P state, and to the $1p_{\Xi^-}$ nuclear state that started as atomic 2P state are found comparable to each other, accounting together for 7.6% of the total 3D width $\Gamma_{3\text{D}} = 3.93$ eV as obtained using the optical potential (3). However, the subsequent $\Xi^- p \rightarrow \Lambda\Lambda$ capture will proceed preferentially from the $1p_{\Xi^-}$ nuclear state that offers good overlap between the $1p_{\Xi^-}$ and $1p_p$ valence-proton orbits. Since the final $1s_{\Lambda}^2$ configuration has $J_f = 0$, and the p -shell protons in ^{12}C are mostly in $j = \frac{3}{2}$ orbits, the requirement $J_i = J_f = 0$ imposes $j_{\Xi^-} = \frac{3}{2}$ on the spin-orbit doublet members of the $1p_{\Xi^-}$ state. The shift of this $1p_{\Xi^-}(\frac{3}{2})$ sub level from the $1p_{\Xi^-}$ $(2j+1)$ -average is estimated, based on the 152 keV $1p_{\Lambda}$ spin-orbit splitting observed in $^{13}_{\Lambda}\text{C}$ [38] to be less than 100 keV upward [39] and, hence, within the 0.15 MeV listed uncertainty introduced here for the position of the $(2j+1)$ -averaged $1p_{\Xi^-}$ state.

4. Spectroscopy of $^{14}\text{N}_{\text{g.s.}} + 1p_{\Xi^-}$ states

Having derived the strength parameter $\text{Re } b_0 = 0.32 \pm 0.01$ fm of V_{opt} by fitting it to $B_{\Xi^-}^{1p}(^{12}\text{C}) = 0.82 \pm 0.15$ MeV, we apply this optical potential to ^{14}N where it yields $B_{\Xi^-}^{1p}(^{14}\text{N}) = 2.08 \pm 0.28$ MeV, considerably higher than the value $B_{\Xi^-} = 1.15 \pm 0.20$ MeV obtained from the three events assigned in Table 1 to Ξ^- capture in ^{14}N . However, this calculated $B_{\Xi^-}^{1p}(^{14}\text{N})$ corresponds to a $(2\mathcal{L}+1)$ -average of binding energies for a triplet of states $\mathcal{L}^{\pi} = (0^-, 1^-, 2^-)$

obtained by coupling a $1p_{\Xi^-}$ state to $J^\pi(^{14}\text{N}_{\text{g.s.}})=1^+$, as shown in Fig. 2. We now discuss the splitting of these triplet states. Effects of Ξ^- Pauli spin, $s_{\Xi^-} = \frac{1}{2}$, are introduced at a later stage.

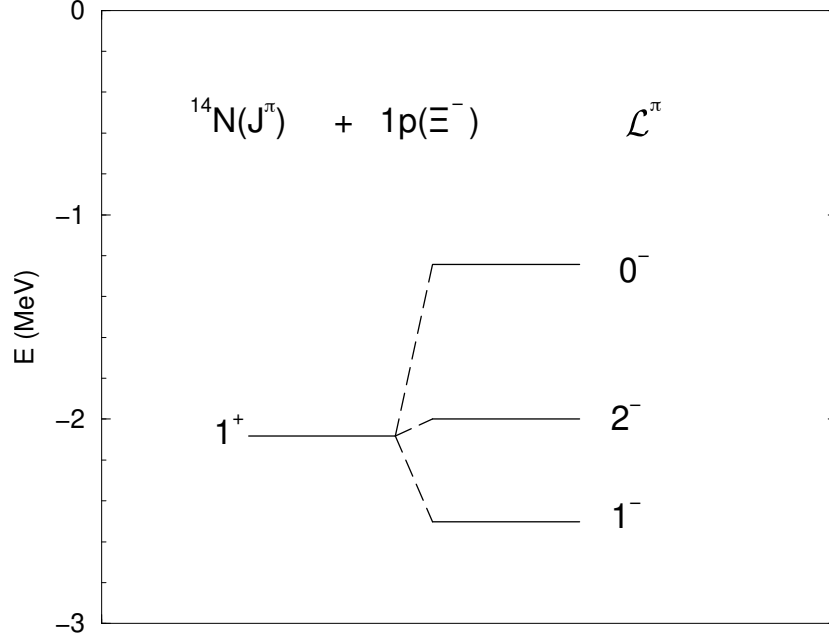


Figure 2: Energies (in MeV) of $\mathcal{L}^\pi = (0^-, 1^-, 2^-)$ triplet of $^{14}\text{N}_{\text{g.s.}} + 1p_{\Xi^-}$ states, split by a $Q_N \cdot Q_\Xi$ residual interaction (5). The $(2\mathcal{L} + 1)$ -averaged energy -2.08 ± 0.28 MeV was calculated using the same optical potential parameter b_0 that yields a $^{12}\text{C}_{\text{g.s.}} + 1p_{\Xi^-}$ state at -0.82 ± 0.15 MeV, corresponding to the Ξ^- capture events in ^{12}C listed in Table 1.

The construction of the $^{14}\text{N}_{\text{g.s.}} + 1p_{\Xi^-}$ spectrum in Fig. 2 follows a similar $^{12}\text{C}(2^+; 4.44 \text{ MeV}) + 1p_\Lambda$ spectrum construction in $^{13}_\Lambda\text{C}$ [40]. The energy splittings marked in the figure are obtained from a two-body spin-independent interaction $V_0(r_{\Xi N})$, Eq. (4), between a p -shell Ξ hyperon and p -shell nucleons, expressed in terms of its shell-model (SM) quadrupole-quadrupole residual interaction $\mathcal{V}_{\Xi N}$,

$$\mathcal{V}_{\Xi N} = F_{\Xi N}^{(2)} Q_N \cdot Q_\Xi, \quad Q_B = \sqrt{\frac{4\pi}{5}} Y_2(\hat{r}_B), \quad (5)$$

where $F^{(2)}$ is the corresponding Slater integral [41]. A representative value of $F_{\Xi N}^{(2)} = -3$ MeV is used here, smaller than the value $F_{\Lambda N}^{(2)} = -3.7$ MeV

established empirically for p -shell Λ hypernuclei [42], in accordance with a ΞN strong interaction somewhat weaker than the ΛN strong interaction (see next section). A single 3D_1 ${}^{14}\text{N}_{\text{g.s.}}$ SM component providing a good approximation to the full SM intermediate-coupling g.s. wavefunction [43] was assumed in the present evaluation.

Fig. 2 exhibits a triplet of ${}^{14}\text{N}_{\text{g.s.}} + 1p_{\Xi^-}$ levels, spread over more than 1 MeV. The least bound triplet state, with $\mathcal{L}^\pi = 0^-$, is shifted upward by 0.84 MeV from the $(2\mathcal{L} + 1)$ averaged position at -2.08 ± 0.28 MeV to $E(0^-) = -1.24 \pm 0.28$ MeV. This is consistent with the averaged position $\bar{E} = -1.15 \pm 0.20$ MeV of the three Ξ^- ${}^{14}\text{N}_{\text{g.s.}}$ capture events listed in Table 1. We are not aware of any good reason why capture has not been seen from the other two states with $\mathcal{L}^\pi = 1^-, 2^-$. This may change when more events are collected at the next stage of the ongoing J-PARC E07 emulsion experiment.

Table 2: Quadrupole-quadrupole contributions to the energies $E(\mathcal{L}^\pi)$ of the ${}^{14}\text{N}_{\text{g.s.}} + 1p_{\Xi^-}$ triplet of states shown in Fig. 2 with respect to $E({}^{14}\text{N}_{\text{g.s.}})$, using $F_{\Xi N}^{(2)} = -3$ MeV, and spin contributions to the splittings $\Delta E(\mathcal{L}) = E(J = \mathcal{L} + \frac{1}{2}) - E(J = \mathcal{L} - \frac{1}{2})$ of the $\mathcal{L} \neq 0$ states. A_{ls} and A_{ss} are spin-orbit ($l_\Xi = 1, s_\Xi = \frac{1}{2}$) and spin-spin ($s_N = s_\Xi = \frac{1}{2}$) energy splittings, respectively, see text.

Interaction	$E(0^-)$	$E(1^-)$	$E(2^-)$	$\Delta E(1^-)$	$\Delta E(2^-)$
$Q_N \cdot Q_\Xi$	$-\frac{7}{25} F_{\Xi N}^{(2)}$	$\frac{7}{50} F_{\Xi N}^{(2)}$	$-\frac{7}{250} F_{\Xi N}^{(2)}$	–	–
$l_\Xi \cdot s_\Xi$	–	–	–	$\frac{1}{2} A_{ls}$	$\frac{5}{6} A_{ls}$
$s_N \cdot s_\Xi$	–	–	–	$\frac{3}{8} A_{ss}$	$\frac{5}{8} A_{ss}$

Introducing Pauli spin, $s_{\Xi^-} = \frac{1}{2}$, the total angular momentum of the uppermost level marked 0^- in Fig. 2 becomes $J^\pi = \frac{1}{2}^-$, but its position is unaffected by spin-orbit and spin-spin interactions. Each of the other two levels in Fig. 2 splits into a doublet $J = \mathcal{L} \pm \frac{1}{2}$ whose $(2J + 1)$ -average remains in the unsplit position. Estimated splittings are listed in Table 2 in terms of two constituent spin matrix elements: $A_{ls} \lesssim 300$ keV [39] for the $l_\Xi \cdot s_\Xi$ spin-orbit splitting $E_{1p_\Xi}(\frac{3}{2}^-) - E_{1p_\Xi}(\frac{1}{2}^-)$, and $A_{ss} \approx 400 \pm 80$ keV for the $s_N \cdot s_\Xi$ spin-spin splitting $E(S_{\Xi N} = 0) - E(S_{\Xi N} = 1)$ for p -shell nucleon and Ξ hyperon. For estimating A_{ss} we used the HAL-QCD [5] volume integral of V_σ , Eq. (4), relative to that of V_0 , thereby generating about 20% systematic uncertainty. Incorporating these spin splittings into the $\mathcal{L}^\pi = (0^-, 1^-, 2^-)$ triplet in Fig. 2 keeps the $\mathcal{L}^\pi = 0^-$ state of interest, which has become $J^\pi = \frac{1}{2}^-$, well separated by at least 0.5 MeV from the rest of the split states.

5. Density dependence, Ξ nuclear potential depth and $1s_{\Xi^-}$ states

So far we have discussed a density independent t -matrix element b_0 in V_{opt} , Eq. (3), to fit the Ξ^- capture events in ^{12}C from Table 1. The resulting value $\text{Re } b_0 = 0.32 \pm 0.01$ fm implies, in the limit $A \rightarrow \infty$ and $\rho(r) \rightarrow \rho_0 = 0.17 \text{ fm}^{-3}$, a value $V_{\Xi} = 24.3 \pm 0.8$ MeV in nuclear matter, in accordance with the extraction of V_{Ξ} from old emulsion events [9] but exceeding considerably other values reviewed in the Introduction. To explore how robust this conclusion is, we introduce the next to leading-order density dependence of V_{opt} , replacing $\text{Re } b_k$ ($k=0,1$) in Eq. (3) by

$$\text{Re } b_k(\rho) = \frac{\text{Re } b_k}{1 + \frac{3k_F}{2\pi} \text{Re } b_0^{\text{lab}}}, \quad k_F = (3\pi^2 \rho/2)^{\frac{1}{3}}, \quad (6)$$

where k_F is the Fermi momentum corresponding to nuclear density ρ and $b_0^{\text{lab}} = (1 + \frac{m_{\Xi^-}}{m_N})b_0$ is the lab transformed form of the c.m. scattering amplitude b_0 . Eq. (6) accounts for Pauli exclusion correlations in ΞN in-medium multiple scatterings [26, 44]. Variants of the form (6) have been used in kaonic atoms [45] and mesic nuclei [46, 47, 48] calculations. Shorter-range correlations, disregarded here, were shown in Ref. [46] to contribute less than $\sim 30\%$ of the long-range Pauli correlation term. Applying Eq. (6) in the present context, $B_{\Xi^-}^{1p} (^{12}\text{C}) = 0.82$ MeV is refitted by $\text{Re } b_0 = 0.527$ fm, lowering the former value $B_{\Xi^-}^{1p} (^{14}\text{N}) = 2.08$ MeV to 1.95 MeV without any substantive change in the conclusions drawn above regarding the five two-body capture events deciphered here. The nuclear-matter Ξ -nuclear potential depth V_{Ξ} decreases from 24.3 ± 0.8 to 21.9 ± 0.7 MeV, a decrease of merely 10%, with additional systematic uncertainty of less than 1 MeV. This value of V_{Ξ} is sufficient to bind $1s_{\Xi^-}$ states in p -shell nuclei, with systematic uncertainty of less than 0.5 MeV, as demonstrated in Table 3 which shows a steady decrease of $B_{\Xi^-}^{1s}$ and $\Gamma_{\Xi^-}^{1s}$ down to ^4He . The increased $\Gamma_{\Xi^-}^{1s} (^4\text{He})$ reflects a denser ^4He medium. However, expecting corrections of order $\mathcal{O}(1/A)$ to the optical potential methodology, our ^4He result should be taken with a grain of salt. It is worth noting that all listed $1s_{\Xi^-}$ g.s. levels remain bound also when the attractive finite-size Coulomb interaction V_c is switched off. None of such $1s_{\Xi^-}$ states have been observed conclusively in dedicated experiments.

The $T = \frac{1}{2}$ ^{11}B nucleus, the only $T \neq 0$ nucleus listed in Table 3, requires in addition to the isoscalar parameter $b_0 = 0.527 + i0.010$ fm also a knowledge of the isovector parameter b_1 . Here we used the HAL-QCD [5] volume integral of $V_{\tau}(r_{\Xi N})$ relative to that of $V_0(r_{\Xi N})$, Eq. (4), to estimate b_1 relative to

Table 3: Binding energies $B_{\Xi^-}^{1s}$ and widths $\Gamma_{\Xi^-}^{1s}$ (in MeV) in core nuclei ${}^AZ(J_c)$, g.s. spin J_c , obtained by solving Eq. (2) with $b_0 = 0.527 + i0.010$ fm and $b_1 = -0.225$ fm in V_{opt} , Eqs. (3),(6). A finite-size Coulomb interaction V_c is included.

	${}^{14}\text{N}(1)$	${}^{12}\text{C}(0)$	${}^{11}\text{B}(\frac{3}{2})$	${}^{10}\text{B}(3)$	${}^6\text{Li}(1)$	${}^4\text{He}(0)$
$B_{\Xi^-}^{1s}$	11.5	9.8	8.4	7.6	2.1	2.0
$\Gamma_{\Xi^-}^{1s}$	1.02	0.93	0.89	0.77	0.26	0.45

b_0 , thereby deriving a value $b_1 = -0.225$ fm.² The resulting value $B_{\Xi^-}^{1s}({}^{11}\text{B})$ listed in the table is lower by 530 keV than obtained disregarding b_1 . Next, we introduce $s_{\Xi^-} = \frac{1}{2}$ Pauli spin, splitting each of the listed $1s_{\Xi^-}$ levels in $J_c \neq 0$ core nuclei into two sub levels $J = J_c \pm \frac{1}{2}$. Using HAL-QCD [5] ratios of volume integrals of $V_{\sigma}(r_{\Xi N})$ and $V_{\sigma\tau}(r_{\Xi N})$ to that of $V_0(r_{\Xi N})$, Eq. (4), as done above for V_{τ} , we estimate the $1s_{\Xi^-}$ spin splittings to be well below 1 MeV. Other potential sources of Ξ^- spin splittings that are relevant in Λ hypernuclei, such as tensor or induced nuclear spin-orbit terms, are likely to be considerably weaker than evaluated in Ref. [49] and are disregarded here. Of particular interest is the $({}^{11}\text{B}_{\text{g.s.}} + 1s_{\Xi^-})$ $J^{\pi} = 1^-$ doublet member expected to be formed in the ${}^{12}\text{C}(K^-, K^+)$ production reaction when the outgoing K^+ meson is detected in the forward direction. Our estimates place it about 0.5 MeV deeper than the listed $(2J+1)$ -averaged $B_{\Xi^-}^{1s}({}^{11}\text{B})=8.4$ MeV, contrasting statements, e.g. [8], that adopt $B_{\Xi^-}^{1s}({}^{11}\text{B})\sim 5$ MeV from the BNL AGS-E885 ${}^{12}\text{C}(K^-, K^+)$ experiment [13]. In fact, the E885 poor resolution prevents making any such conclusive statement.

6. Conclusion

We have shown that all five light nuclear emulsion events identified in KEK and J-PARC K^- exposure experiments as two-body Ξ^- capture in ${}^{12}\text{C}$ and ${}^{14}\text{N}$ into twin Λ hypernuclei correspond to capture from $1p_{\Xi^-}$ Coulomb-assisted bound states. This involved using just one *common* strength parameter of a density dependent optical potential. Long-range ΞN shell-model correlations were essential in making the ${}^{14}\text{N}$ events consistent with the ${}^{12}\text{C}$ events. Earlier attempts to explain these data overlooked this point, therefore

²Note that $\text{Im } b_1 = 0$ because the charge exchange $\Xi^- + {}^{11}\text{B} \rightarrow \Xi^0 + {}^{11}\text{Be}$ is kinematically blocked.

reaching quite different conclusions [50, 51, 52, 53, 54]. Predicted then are $1s_{\Xi^-}$ bound states with $B_{\Xi^-}^{1s} \sim 10$ MeV in ^{12}C and somewhat larger in ^{14}N , deeper by 4–5 MeV than the $1s_{\Xi^-}$ states claimed by a recent J-PARC E07 report of multibody capture events [24]. The Ξ nuclear-matter potential depth derived here within an optical potential methodology, $V_{\Xi} = 21.9 \pm 0.7$ MeV, is considerably larger than G -matrix values below 10 MeV derived from recent LQCD and EFT ΞN potentials [27, 29]. A systematic optical-potential model uncertainty of less than 1 MeV as discussed in Sect. 5 is short of bridging the gap noted above. Substantial ΞNN three-body *attractive* contributions to the Ξ nuclear potential depth would be required to bridge this gap. Intuitively one expects repulsive BNN three-body contributions for octet baryons B , e.g. Ref. [31], but in chiral EFT studies, focusing on decuplet- B^* intermediate B^*NN and $BN\Delta$ configurations, this has been proven so far only for $B = \Lambda$ [55, 56].

To check the procedure practised in Sect. 5 for fitting V_{Ξ} to just one Ξ^- - ^{12}C bound state datum, we apply it to the $1s_{\Lambda}$ binding energy in ^{12}C , $B_{\Lambda}^{1s} = 11.69 \pm 0.12$ MeV [57]. The fitted strength $b_0 = 0.866 \pm 0.010$ fm amounts to a nuclear-matter Λ potential depth $V_{\Lambda} = 31.7 \pm 0.2$ MeV, in good agreement with the accepted value $V_{\Lambda} \approx 30$ MeV [7]. One may slightly improve the derived value of V_{Λ} by subtracting from B_{Λ}^{1s} a nuclear induced spin-orbit contribution that vanishes in the limit $A \rightarrow \infty$, thereby reducing our input B_{Λ}^{1s} to 10.85 MeV [49]. This gives $b_0 = 0.798 \pm 0.010$ fm and $V_{\Lambda} = 30.5 \pm 0.2$ MeV. Here too it is not possible to separate the contribution of ΛNN three-body potential terms from that of the main ΛN two-body potential term.

A strong Ξ -nuclear interaction, such as derived here, may have far-reaching implications to (N, Λ, Ξ) strange hadronic matter [10] and particularly to dense neutron star matter [11]. In the latter case a strong Ξ -nuclear interaction might cause a faster depletion of Λ hyperons by $\Lambda\Lambda \rightarrow \Xi^- p$, a process inverse to the Ξ^- capture reaction considered in the present work. More work is necessary in this direction.

Acknowledgments

Recent related correspondence with Johan Haidenbauer, Jiří Mareš, John Millener, Tomofumi Nagae, Josef Pochodzalla and Tom Rijken is gratefully acknowledged. The present work is part of a project funded by the European

Union's Horizon 2020 research & innovation programme, grant agreement 824093.

References

- [1] S. Acharya, et al. (ALICE Collaboration), Phys. Rev. C 99 (2019) 024001.
- [2] S. Acharya, et al. (ALICE Collaboration), Phys. Lett. B 797 (2019) 134822.
- [3] S. Acharya, et al. (ALICE Collaboration), Phys. Rev. Lett. 123 (2019) 112002.
- [4] S. Acharya, et al. (ALICE Collaboration), Nature 588 (2020) 232.
- [5] K. Sasaki, et al. (HAL QCD Collaboration), Nucl. Phys. A 998 (2020) 121737.
- [6] L. Tolos, L. Fabbietti, Prog. Part. Nucl. Phys. 112 (2020) 103770.
- [7] A. Gal, E.V. Hungerford, D.J. Millener, Rev. Mod. Phys. 88 (2016) 035004.
- [8] E. Hiyama, K. Nakazawa, Annu. Rev. Nucl. Part. Sci. 68 (2018) 131.
- [9] C.B. Dover, A. Gal, Ann. Phys. 146 (1983) 309.
- [10] J. Schaffner-Bielich, A. Gal, Phys. Rev. C 62 (2000) 034311, and references cited therein to earlier work.
- [11] S. Weissenborn, D. Chatterjee, J. Schaffner-Bielich, Nucl. Phys. A 881 (2012) 62.
- [12] T. Fukuda, et al. (E224 Collaboration), Phys. Rev. C 58 (1998) 1306.
- [13] P. Khaustov, et al. (The AGS E885 Collaboration), Phys. Rev. C 61 (2000) 054603.
- [14] T. Harada, Y. Hirabayashi, Phys. Rev. C 103 (2021) 024605.
- [15] J.K. Ahn, et al., Phys. Rev. Lett. 87 (2001) 132504.

- [16] T. Nagae, et al., AIP Conf. Proc. 2130 (2019) 020015.
- [17] J. Pochodzalla, et al. (for the PANDA Collaboration), JPS Conf. Proc. 17 (2017) 091002.
- [18] C.Z. Yuan, M. Karliner, Phys. Rev. Lett. 127 (2021) 012003.
- [19] C.J. Batty, E. Friedman, A. Gal, Phys. Rev. C 59 (1999) 295.
- [20] D. Zhu, C.B. Dover, A. Gal, M. May, Phys. Rev. Lett. 67 (1991) 2268.
- [21] S. Aoki, et al. (KEK E176 Collaboration), Nucl. Phys. A 828 (2009) 191, and earlier E176 publications cited therein.
- [22] H. Nakazawa, et al. (KEK PS-E373), Prog. Theor. Exp. Phys. 2015 (2015) 033D02.
- [23] S.H. Hayakawa, et al. (J-PARC E07 Collaboration), Phys. Rev. Lett. 126 (2021) 062501.
- [24] M. Yoshimoto, et al. (J-PARC E07), Prog. Theor. Exp. Phys. 2021 (2021) 073D02.
- [25] T. Koike, JPS Conf. Proc. 17 (2017) 033011.
- [26] C.B. Dover, J. Hüfner, R.H. Lemmer, Ann. Phys. 66 (1971) 248.
- [27] T. Inoue (for HAL QCD Collaboration), AIP Conf. Proc. 2130 (2019) 020002.
- [28] J. Haidenbauer, U.-G. Meißner, Eur. Phys. J. A 55 (2019) 23.
- [29] M. Kohno, Phys. Rev. C 100 (2019) 024313.
- [30] T. Gaitanos, A. Choroziadou, Nucl. Phys. A 1008 (2021) 122153.
- [31] M.M. Nagels, Th.A. Rijken, Y. Yamamoto, Phys. Rev. C 102 (2020) 054003; see in particular Tables XXI, XXIV for models ESC16*(A,B) respectively.
- [32] E. Friedman, A. Gal, Phys. Rep. 452 (2007) 89.
- [33] L.R.B. Elton, *Nuclear Sizes*, (Oxford Univ. Press, Oxford, 1961).

- [34] I. Angeli, K.P. Marinova, *At. Data Nucl. Data Tables* 99 (2013) 69.
- [35] C.W. de Jager, H. de Vries, C. de Vries, *At. Data Nucl. Data Tables* 14 (1974) 479.
- [36] H. de Vries, C.W. de Jager, C. de Vries, *At. Data Nucl. Data Tables* 36 (1987) 495.
- [37] A. Gal, E. Friedman, C.J. Batty, *Nucl. Phys. A* 606 (1996) 283.
- [38] S. Ajimura, et al., *Phys. Rev. Lett.* 86 (2001) 4255.
- [39] J. Mareš, B.K. Jennings, *Phys. Rev. C* 49 (1994) 2472.
- [40] E.H. Auerbach, A.J. Baltz, C.B. Dover, A. Gal, S.H. Kahana, L. Ludeking, D.J. Millener, *Phys. Rev. Lett.* 47 (1981) 1110, *Ann. Phys.* 148 (1983) 381 where values of $-F_{\Lambda N}^{(2)} = 3.0 - 3.4$ MeV were proposed.
- [41] A. de-Shalit, I. Talmi, *Nuclear Shell Theory* (AP, New York, 1963).
- [42] R.H. Dalitz, A. Gal, *Ann. Phys.* 131 (1981) 314.
- [43] D.J. Millener, in *Topics in Strangeness Nuclear Physics*, Edited by P. Bydžovský, A. Gal, and J. Mareš, *Lecture Notes in Physics* 724 (Springer, Heidelberg, 2007) 31-79.
- [44] T. Waas, M. Rho, W. Weise, *Nucl. Phys. A* 617 (1997) 449.
- [45] E. Friedman, A. Gal, *Nucl. Phys. A* 899 (2013) 60, *Nucl. Phys. A* 959 (2017) 66.
- [46] W. Weise, R. Härtle, *Nucl. Phys. A* 804 (2008) 173.
- [47] E. Friedman, A. Gal, J. Mareš, *Phys. Lett. B* 725 (2013) 334.
- [48] A. Cieplý, E. Friedman, A. Gal, J. Mareš, *Nucl. Phys. A* 925 (2014) 126.
- [49] D.J. Millener, *Nucl. Phys. A* 881 (2012) 298.
- [50] M. Yamaguchi, K. Tominaga, Y. Yamamoto, T. Ueda, *Prog. Theor. Phys.* 105 (2001) 627.
- [51] E. Hiyama, Y. Yamamoto, H. Sagawa, *Phys. Scr.* 91 (2016) 093001.

- [52] T.T. Sun, E. Hiyama, H. Sagawa, H.-J. Schulze, J. Meng, Phys. Rev. C 94 (2016) 064319.
- [53] J. Hu, H. Shen, Phys. Rev. C 96 (2017) 054304.
- [54] Y. Jin, X.-R. Zhou, Y.-Y. Cheng, H.-J. Schulze, Eur. Phys. J. A 56 (2020) 135.
- [55] S. Petschauer, J. Haidenbauer, N. Kaiser, U.-G. Meißner, W. Weise, Nucl. Phys. A 957 (2017) 347.
- [56] D. Gerstung, N. Kaiser, W. Weise, Eur. Phys. J. A 56 (2020) 175.
- [57] D.H. Davis, Nucl. Phys. A 754 (2005) 3c.